Biotechnology Reports 42 (2024) e00841

Contents lists available at ScienceDirect

Biotechnology Reports

journal homepage: www.elsevier.com/locate/btre

Research Article

Characterization of plant produced V_{HH} antibodies against cobra venom toxins for antivenom therapy

Sarocha Vitayathikornnasak [a], Kaewta Rattanapisit [b], Ashwini Malla [b], Pipob Suwanchaikasem [b], Richard Strasser [d], Narach Khorattanakulchai [b], Kanokporn Pothisamutyothin [e], Wanatchaporn Arunmanee [e,f], Waranyoo Phoolcharoen [a,c,*]

[a] Faculty of Pharmaceutical Sciences, Chulalongkorn University, Bangkok, Thailand
[b] Baiya Phytopharm Co., Ltd., Bangkok, Thailand
[c] Center of Excellence in Plant-Produced Pharmaceuticals, Chulalongkorn University, Bangkok, Thailand
[d] Department of Applied Genetics and Cell Biology, Institute of Plant Biotechnology and Cell Biology, University of Natural Resources and Life Sciences, Vienna, Vienna, Austria
[e] Department of Biochemistry and Microbiology, Faculty of Pharmaceutical Sciences, Chulalongkorn University, Bangkok, Thailand
[f] Center of Excellence in Cancer Cell and Molecular Biology, Faculty of Pharmaceutical Sciences, Chulalongkorn University, Bangkok, Thailand

ARTICLE INFO

Keywords:
Single variable domain (V_{HH})
Cobra venom
A-neurotoxin
Phospholipase A2
Nicotiana benthamiana
Plant produced antibody
Heavy chain antibody (HCAb)

ABSTRACT

Cobra (*Naja kaouthia*) venom contains many toxins including α-neurotoxin (αNTX) and phospholipase A2 (PLA2), which can cause neurodegeneration, respiratory failure, and even death. The traditional antivenom derived from animal serum faces many challenges and limitations. Heavy-chain-only antibodies (HCAb), fusing V_{HH} with human IgG Fc region, offer advantages in tissue penetration, antigen binding, and extended half-life. This research involved the construction and transient expression of two types of V_{HH}-F_C which are specific to α-Neurotoxin (V_{HH}-αNTX-F_C) and Phospholipase A2 (V_{HH}-PLA2-F_C) in *Nicotiana benthamiana* leaves. The recombinant HCAbs were incubated for up to six days to optimize expression levels followed by purification by affinity chromatography and characterization using LC/Q-TOF mass spectrometry (MS). Purified proteins demonstrated over 92 % sequence coverage and an average mass of around 82 kDa with a high-mannose N-glycan profile. An antigen binding assay showed that the V_{HH}-αNTX-Fc has a greater ability to bind to crude venom than V_{HH}-PLA2-Fc.

1. Background

Snakebite envenomation is a major health problem that leads to physical injury and disability, particularly in regions of Africa, Asia, and Latin America. According to the World Health Organization (WHO), there were an estimated 1.8 – 2.7 million cases of snakebites annually between 2022 and 2023, resulting in serious illness or permanent disabilities. Envenomation causes the death of 81,000 to 138,000 people each year [1]. Snakebites are a severe health problem, especially in the region of South-East Asia, which accounts for almost 70 % of estimated global snakebite deaths [2]. In addition, traditional antivenom produced from animals has limitations, including adverse reactions, low purity of specific antibodies, and a high-cost and time-consuming production process. [3,4]. Therefore, the development of efficient, safe, and affordable antivenom(s) is necessary to protect against and treat snakebites.

The Cobra snake belongs to the "*Naja*" genus and is a member of the *Elapidae* family of snakes. They are widely distributed in Africa and Asia and are responsible for a great number of snake envenomation cases in these continents [5]. Snake venom is composed of many biologically active proteins, with α-Neurotoxin (αNTX) being the major component followed by Phospholipase A2 (PLA2) in Cobra snake venom [6,7]. α-Neurotoxin (αNTX) belongs to the three-finger toxin (3FTx) group, which is the most important group exerting neurotoxic effects by interacting with muscle nicotinic cholinergic receptors (nAChRs), causing lethality [8]. Neurotoxins in cobra venom can vary in terms of measure and potency in different species and their geographical locations [7,9,10]. Phospholipase A2 (PLA2) enzymes also play a major role in the neurotoxic and myotoxic effects after snake bites [11]. PLA2 is an enzymatic toxin found in snake venoms that typically causes damage to

* Corresponding author.
E-mail address: waranyoo.p@chula.ac.th (W. Phoolcharoen).

https://doi.org/10.1016/j.btre.2024.e00841
Received 27 January 2024; Received in revised form 12 April 2024; Accepted 14 April 2024
Available online 16 April 2024

cellular and subcellular membranes, lysis of erythrocytes, blood coagulation, and cardiotoxicity [12]. PLA2 creates cationic channels in cell membranes, leading to flooding of the cells with sodium and calcium ions, which can result in cell death due to calcium intoxication, ionic imbalance, swelling, and cell rupture [13]. Elapid venom consists mainly of 3FTx and PLA2, which make up to 80 % of the total venom proteome. These components are responsible for the neurotoxicity in individuals bitten by cobras [6,7]. As a consequence, cobra envenomation can cause paralysis, respiratory failure, cardiac arrest, and death [14].

Single variable domains (V_{HH}), also known as nanobodies, are naturally found in camelids [15–17]. Due to their small size of around 15 kDa compared to IgG antibodies, V_{HH} are highly effective in binding and neutralizing their targets, allowing for quick diffusion throughout the body to neutralize snake venom toxin proteins that causes tissue damage at the bite site. Moreover, this approach offers many advantages, such as high solubility, tissue permeability, and stability to changes in pH and temperature [16,18,19]. However, due to its small size, V_{HH} is cleared from the bloodstream much faster than larger proteins that are above the glomerular filtration cutoff size of 65 kDa [20]. Therefore, the fusion of the Fc region in heavy-chain-only antibodies (HCAb), which contain two heavy chains, with a single variable domain V_{HH} as the antigen-binding region, could lead to a longer half-life. [20,21]. Chimeric nanobody-heavy chain antibodies have both the advantageous features of nanobodies and human Fc domains by combining V_{HH} with the Fc region of human IgG to enhance their half-life [17,22]. Thus, the recombinant V_{HH}-Fc is a promising candidate for various applications in biomedical research, diagnosis, and therapy.

Currently, plant-based platforms for transient antibody expression have been gaining more attention due to their excellent advantages such as effectiveness, cost-saving, rapid production, and sustainability [23, 24]. Plant-produced monoclonal antibodies (mAbs) have been used for treatment of various infections and diseases such as HIV, breast cancer, influenza, rabies virus, parvo virus, Covid-19, Ebola, and monocytic leukemia [25–31].

The objective of this research was to express V_{HH}-Fc single heavy chain fragments that contain variable heavy chain domains encoding α-Neurotoxin (V_{HH}-αNTX-Fc) and/or Phospholipase A2 (V_{HH}-PLA2-Fc) in *Nicotiana benthamiana*. The combination of fast growth, high biomass production, ease of transformation, high protein expression levels, and compatibility with viral vectors, low nicotine content makes *N. benthamiana* a popular choice for transient expression of recombinant proteins in plants.

The plant-based platform was optimized to achieve the highest yields of V_{HH}-αNTX-Fc and V_{HH}-PLA2-Fc expression by varying the incubation period after days post infiltration. The recombinant proteins were then purified using protein A chromatography, characterized for their structural assembly, and further tested for their antigen binding activity.

2. Methods

2.1. Cloning and transient expression of V_{HH}-αNTX-Fc and V_{HH}-PLA2-Fc gene

The sequence of V_{HH}-αNTX was acquired from United States, (Patent No. US 2013/0259864 A1' Cluster II C2) [22] and that of V_{HH}-PLA2 from a previousstudy by Chavanayarn et al., 2012 [12]. Each of them was codon-optimized for plant and synthesized by Genewiz (Suzhou, China). Each of the llama single variable domain (V_{HH}) genes of αNTX and PLA2 was individually cloned, digested with *Xba*I/*Bam*HI and ligated with constant region of human IgG1 heavy chain CH_2 and CH_3 (Fc, Genbank accession number: 4CDH_A) for cloning into geminiviral vector pBY2eK. The pBY2eK-V_{HH}-Fc were transformed into *Escherichia coli* strain DH10B by heat shock and the recombinant plasmids were confirmed by restriction digestion using enzymes *Xba*I and *Sac*I and further by DNA sequencing. The confirmed plasmids were transformed to *Agrobacterium tumefaciens* GV3101 by electroporation.

Nicotiana benthamiana plants were grown under controlled conditions with 8-h dark/16-h light cycle for 6 – 8 weeks. *A. tumefaciens* GV3101 containing pBY2eK-V_{HH}-αNTX-Fc and pBY2eK-V_{HH}-PLA2-Fc were separately grown in Luria–Bertani (LB) broth with 1 mg/L kanamycin, 1 mg/L gentamycin, 1 mg/L rifampicin at 28 °C overnight with shaking at 200 rpm. Then, the overnight-grown culture was centrifuged at 5000 g for 10 min at 25 °C. The pellet was resuspended in the infiltration buffer [10 mM $MgSO_4$, 10 mM 2-(N-morpholino) ethanesulfonic acid (MES) pH 5.5]. *N. benthamiana* leaves were infiltrated with *A. tumefaciens* GV3101 containing pBY2eK-V_{HH}-αNTX-Fc and pBY2eK-V_{HH}-PLA2-Fc individually, at a final OD_{600} of 0.2 using syringe. Leaf samples were extracted with 1X PBS (phosphate-buffered saline: 137 mM NaCl, 2.7 mM KCl, 4.3 mM Na_2HPO_4, 1.47 mM KH_2PO_4), pH 7.4. The expression of V_{HH}-αNTX-Fc and V_{HH}-PLA2-Fc in *N. benthamiana* leaves were determined by SDS-PAGE and western blot. All crude proteins were loaded equally at a concentration of 15 μg/well to compare the band intensity using ImageQuant™ (Biorad, California, USA). The crude protein extracts were estimated for total protein by Bradford reagent (Bio-rad, California, USA) method using bovine serum albumin (BSA) as a standard (Thermo Scientific, Illinois, USA).

2.2. Purification of plant-produced V_{HH}-αNTX-Fc and V_{HH}-PLA2-Fc

Infiltrated *N. benthamiana* leaves were extracted with 1X PBS, pH 7.4 using a blender (JSR, Gongju-si, Korea) and centrifuged (Thermo Scientific, Massachusetts, USA) at 26,000 g for 30 min. The supernatant was filtered with a 0.45 μm membrane filter (Pall Corporation, New York, USA) and loaded onto a protein-A affinity column. The column was washed with ten-column volumes of PBS pH 7.4. The bound protein was eluted with 0.1 M glycine (Vivantis, Shah Alam, Malaysia), pH 2.7, and rapidly neutralized to pH 7.4 with 1.5 M Tris–HCl (Vivantis, Shah Alam, Malaysia), pH 8.8. The purified plant-produced V_{HH}-αNTX-Fc and V_{HH}-PLA2-Fc antibody was analyzed using SDS-PAGE and immunoblot analysis.

2.3. Sodium dodecyl sulfate polyacrylamide gel electrophoresis (SDS-PAGE) and western blot analysis

The plant crude extract or purified plant-produced proteins were further analyzed by SDS-PAGE and Western blot. For crude plant extracts, proteins were separated by SDS-PAGE gradient gel (4–15 %) under non-reducing and reducing conditions using wild type *N. benthamiana* extract as the negative control. The separated proteins were stained with InstantBlue® (Abcam, Cambridge, UK) for proteins visualization and also transferred to nitrocellulose membrane (Bio-Rad, California, USA) for immunoblotting. The membranes were blocked with 5 % skim milk and probed with horseradish peroxidase (HRP)-conjugated goat anti-human IgG (Southern Biotech, Alabama, USA) that was diluted 1:4000 in 3 % skim milk. The membranes were washed three times with 1X PBST (1X PBS with 0.05 % Tween 20 (Sigma-Aldrich, Darmstadt, Germany)) and once with 1X PBS. Then, the membrane was detected for the chemiluminescence signal using ECL detection reagent (Thermoscientific, USA) as per manufacturer's instructions.

2.4. Molecular weight determination by intact protein analysis

For intact structure and mass analysis, 25 μg of V_{HH}-Fc purified proteins were desalted and buffer exchanged with 50 mM ammonium bicarbonate (Honeywell, North Carolina, USA) using a desalting column with MW cut-off at 6000 Da (Bio-Rad, USA). Then, the collected sample was centrifuged at 12,000 g for 10 min. Liquid chromatography quadrupole time-of-flight mass spectrometry (LC/Q-TOF) analysis was conducted on a Liquid Chromatography Mass Spectrometry, Agilent model 6545XT Advance Bio, with a dual Agilent Jet Stream Electrospray Ionization (Dual AJS ESI) source. LC separation was obtained with an

Agilent PLRP-S 1000 Å column (2.1 × 50 mm, 5 μm). Approximately 1 μg of sample was injected for each analysis. The column temperature was set to 60 °C with a flow rate of 0.3 mL/min during sample analysis. 0.1 % formic acid in water and 0.1 % acetonitrile were used as solvents A and B, respectively. The elution gradient duration was 12 min following these different steps: 0–1 min, 25–30 % of B; 1–3 min, 30–32 % of B; 3–4 min, 32–35 % of B; 4–5 min,35–60 % of B; 5–6, 60–90 % of B; 6–9 min, 90 % of B; 9–10 min, 90–25 % of B; 10–12, 25 % of B. The mass spectrometer acquisition parameters were: positive mode, 5000 V capillary voltage, 2000 V nozzle voltage, full scan MS *m/z* @ 10,000–30,000 with a resolution of 2 GHz in MS, collision energy 0 eV. The data obtained from LC/Q-TOF were analyzed using Agilent Mass Hunter Bio Confirm Software version 11.0.

2.5. Subunit protein analysis

For subunit protein analysis, 25 μg of V_{HH}-Fc purified protein was desalted, and buffer exchanged with 50 mM ammonium bicarbonate (Honeywell, North Carolina, USA) using a desalting column with MW cut-off at 6000 Da (Bio-Rad, USA). 100 mM dithiothreitol (DTT) (Glentham Life Sciences, Corsham, UK) was added into sample and incubated at 65 °C for 30 min. Then, the collected sample was centrifuged at 12,000 g for 10 min. The sample was collected using peptide compatible vials. LC/Q-TOF analysis were conducted on a Quadrupole Time of Flight Liquid Chromatography Mass Spectrometry, Agilent model 6545XT Advance Bio, Dual Agilent Jet Stream Electrospray Ionization (Dual AJS ESI) source. LC separation was obtained with an Agilent PLRP-S 1000 Å column (2.1 × 50 mm, 5 μm). Approximately 1 μg of sample was injected for each analysis. The column temperature was set to 60 °C with a flow rate of 0.3 mL/min during sample analysis. 0.1 % formic acid in water and 0.1 % acetonitrile were used as solvents A and B, respectively. The elution gradient duration was 12 min following these different steps: 0–1 min, 25–30 % of B; 1–3 min, 30–32 % of B; 3–4 min, 32–35 % of B; 4–5 min, 35–60 % of B; 5–6, 60–90 % of B; 6–9 min, 90 % of B; 9–10 min, 90–25 % of B; 10–12, 25 % of B. The mass spectrometer acquisition parameters were: Positive mode, 5000 V capillary voltage, 2000 V nozzle voltage, full scan MS *m/z* @ 400–3200 with a resolution of 4 GHz in MS, Collision energy 10 eV. The data obtained from LC/Q-TOF were analyzed using Agilent Mass Hunter Bio Confirm Software version 11.0.

2.6. Protein identification by peptide mapping

Twenty-five μg of V_{HH}-Fc purified protein was desalted and buffer exchanged with 50 mM ammonium bicarbonate (Honeywell, North Carolina, USA) using a desalting column with MW cut-off at 6000 Da (Bio-Rad, USA). 100 mM dithiothreitol (DTT) (Glentham Life Sciences, Corsham, UK) were added and samples were incubated at 65 °C for 30 min. 10 μL of iodoacetamide (IAA) (Glentham Life Sciences, Corsham, UK) was added and the samples were incubated in the dark at room temperature for 20 min. 0.5 μg of trypsin was added to digest the sample and incubated for 4 h. Then, the sample was collected and centrifuged at 12,000 g for 10 min. The sample was collected using peptide compatible vials. LC/Q-TOF analysis was conducted on a Quadrupole Time of Flight Liquid Chromatography Mass Spectrometry, Agilent model 6545XT Advance Bio, with dual Agilent jet stream electrospray ionization (Dual AJS ESI) source. LC separation was obtained with an Agilent Advance Bio Peptide Mapping Column (2.1 × 150 mm, 2.7 μm.) Approximately 1 μg of sample was injected for each analysis. The column temperature was set to 60 °C with a flow rate of 0.4 mL/min during sample analysis. 0.1 % formic acid in water and 0.1 % acetonitrile were used as solvents A and B, respectively. The elution gradient duration was 85 min following these different steps: 0–2 min, 0 % of B; 2–35 min, 0–20 % of B; 35–55 min, 20–30 % of B; 55–65 min, 30–50 % of B; 65–70, 50–90 % of B; 70–75 min, 90 % of B; 75–80 min, 90–0 % of B; 80–85, 0 % of B. The mass spectrometer acquisition parameters were: Positive mode, 4000 V capillary voltage, 500 V nozzle voltage, full scan MS *m/z* @ 100–3000 with a resolution of 2 GHz in MS, Collision energy as formula 3.1 × (*m/z*)/100 – 1 for charge1 – 2; 3.6 × (*m/z*)/100 – 4.8 for charge 3 and >3. The data obtained from LC/Q-TOF were analyzed using Agilent Mass Hunter Bio Confirm Software version 11.0.

2.7. V_{HH}-αNTX-Fc and V_{HH}-PLA2-Fc antigen-binding ELISA

A 96-well ELISA plate (Corning, New York, USA) was coated with 100 μL of 2 μg/mL crude venom of Thailand *Naja kaouthia* (Queen Saovabha Memorial Institute, Thailand) and incubated overnight at 4°C. The coated plate was washed three times with 1X PBST and blocked with 5 % (w/v) BSA for 1 h at 37°C. Then, the plate was washed three times with 1X PBST and incubated with 0.02–240.00 μg/mL (0.000 – 15 μMolar) of purified plant-produced V_{HH}-αNTX-Fc and V_{HH}-PLA2-Fc protein for 1 h at 37°C. The plate was washed three times with 1X PBST and incubated with HRP-conjugated goat anti-human IgG diluted 1:2000 in 1X PBS for 1 h at 37°C. The plate was washed, and the signal was detected with 100 μL of TMB substrate (Promega, USA) and stopped with 100 μL of 1 M H_2SO_4. The absorbance was measured at 450 nm using a Multimode plate reader (Perkin Elmer, EnsightTM, USA). The experiment was performed in three replicates and the data are presented as mean ± SD.

3. Results

3.1. Cloning and transient expression of V_{HH}-αNTX-Fc and V_{HH}-PLA2-Fc in Nicotiana benthamiana

The sequence of V_{HH}-αNTX was obtained from Richard *et al.*, 2013 [22], while the sequence of V_{HH}-PLA2 was obtained from Chavanayarn *et al.*, 2012 [12]. Synthetic V_{HH}-αNTX-Fc or V_{HH}-PLA2-Fc sequences or the Fc coding sequence were inserted into the pBY2eK expression vector using, *Xba*I and *Sac*I restriction enzyme sites (Fig. 1). Each type of V_{HH}-Fc was expressed in 6 – 8 week-old *N. benthamiana* after transformation with *Agrobacterium* harboring the respective pBY2eK-V_{HH}-Fc recombinant vectors and incubated for 6 days after syringe infiltration. Leaves were then extracted and crude extracts were analyzed by SDS-PAGE followed by Western blotting. The expected protein band at around 80 kDa was observed in the infiltrated leaf extracts, whereas no band was observed in the wild type leaf extract, as shown in Fig. 2. The result indicated that *N. benthamiana* successfully expressed both V_{HH}-αNTX-Fc and V_{HH}-PLA2-Fc. Further optimization of the incubation time after infiltration of V_{HH}-αNTX-Fc and V_{HH}-PLA2-Fc into *N. benthamiana* was investigated for 3 replicates. The extracted protein was analyzed by Western blotting using equal amounts of total soluble protein (15 μg). The result showed different band intensities as shown in Fig. 3C – D and Supplemental Figs. S3A – F. V_{HH}-αNTX-Fc showed increased expression and reached the highest level at day 6, whereas the expression of V_{HH}-PLA2-Fc was approximately the same level from day 2 to day 6 (Fig. 3E). However, both proteins showed a decrease in expression after 6 days.

3.2. Purification of V_{HH}-αNTX-Fc and V_{HH}-PLA2-Fc from N. benthamiana leaves

N. benthamiana leaves were infiltrated *via.*, syringe infiltration with V_{HH}-Fc and incubated for 6 days. As shown in Fig. 3A – B, the area of leaf infiltrated with V_{HH}-αNTX-Fc and V_{HH}-PLA2-Fc exhibited curling, and necrosis in comparison with the non-infiltrated area of the leaf. Plant-produced V_{HH}-αNTX-Fc and V_{HH}-PLA2-Fc proteins were expressed and purified by affinity chromatography using Protein A resin (Figure S1 and S2). As shown in Fig. 4A, SDS-PAGE under non-reducing condition showed that both V_{HH}-αNTX-Fc and V_{HH}-PLA2-Fc had a band size around 80 kDa, while a weaker band around 160 kDa may be related to protein aggregates. Under reducing conditions (Fig. 4C), a major band

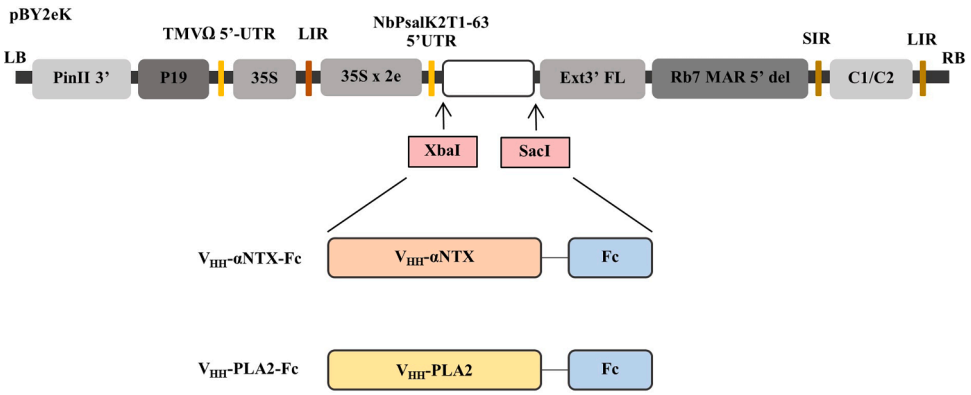

Fig. 1. Illustration of the V_{HH}-αNTX-Fc and V_{HH}-PLA2-Fc expression construct in the pBY2eK geminiviral vector. The vector includes the long intergenic region (LIR) of the bean yellow dwarf virus (BeYDV) genome, the short intergenic region (SIR) of the BeYDV genome, C2/C1 open reading frames coding for the replication initiation proteins Rep and RepA, the 5′ untranslated region (5′UTR) of NbPsaIK2T1–63 and the 30 full length extension gene (Ext3'FL), the p19 gene from tomato bushy stunt virus, the tobacco RB7 promoter (Rb7 MAR 5′ del), the 5′ untranslated region of tobacco mosaic virus Ω (TMVΩ 5′) and the terminator from the potato proteinase inhibitor II gene(Pin II 3′).

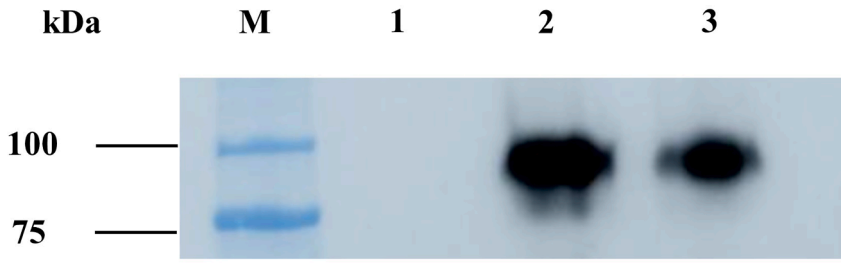

Fig. 2. Western blot analysis of crude extracts containing plant-produced V_{HH}-αNTX-Fc and V_{HH}-PLA2-Fc expressing plants. Crude protein extracts were separated by 4–15 % SDS-PAGE, transferred to nitrocellulose membrane and probed with horseradish peroxidase (HRP)-conjugated goat anti-human IgG. M: Marker (Bio-Rad, California, USA); Lane 1: crude extract from wild type leaves of *Nicotiana benthamiana*; Lane 2: crude extract containing plant-produced V_{HH}-αNTX-Fc; Lane 3: crude extract containing plant-produced V_{HH}-PLA2-Fc.

around 40 kDa was observed, while bands smaller than 40 kDa might correspond to degraded proteins. Furthermore, the result of Western blot analysis was consistent with the result of SDS-PAGE. Both V_{HH}-αNTX-Fc and V_{HH}-PLA2-Fc showed bands specific for anti-human IgG1 Fc gamma at around 80 and 160 kDa under non-reducing conditions (Fig. 4B). Under reducing conditions (Fig 4D), the major band was observed at around 40 kDa. After purification, the average yield of V_{HH}-αNTX-Fc and V_{HH}-PLA2-Fc produced in *N. benthamiana* was observed to be 18.49 and 29.54 μg/g fresh leaf weight, respectively.

3.3. Characterization of V_{HH}-αNTX-Fc and V_{HH}-PLA2-Fc using Lc/Q-Tof

The human Fc domain, which is the scaffold of V_{HH}-Fc fusion proteins contain one N-glycosylation site, located at N223 and N224 of V_{HH}-αNTX-Fc and V_{HH}-PLA2-Fc proteins, respectively. To characterize the N-glycan profiles and confirm the protein masses, plant-produced V_{HH}-αNTX-Fc and V_{HH}-PLA_2-Fc proteins were analyzed in three LC-MS modes: intact protein, subunit protein and peptide mapping.

The intact protein results indicated that the experimental average masses of the non-glycosylated V_{HH}-αNTX-Fc and V_{HH}-PLA2-Fc proteins were 82,858.9724 Da and 82,839.6799 Da, respectively. These values differed from their theoretical masses of 82,861.2974 and 82,837.3093 Da by 2.32 and 2.37 Da, respectively (Supplementary Fig. S4A – B). The glycosylated forms of V_{HH}-αNTX-Fc and V_{HH}-PLA2-Fc proteins were also observed. The most-abundant glycosylated forms were Man8GlcNAc2 glycans attached on both sides of Fc regions, in which their observed masses were 86,264.5941 and 86,241.2449 Da for V_{HH}-αNTX-Fc and V_{HH}-PLA2-Fc, respectively. Additionally, glycans from a pair of attached Man7GlcNAc2, Man8GlcNAc2 or Man9GlcNAc2 glycans were detected (Supplementary Fig. S4A – B). The observation of high-mannose glycosylated forms was a result of adding the KDEL sequence at the C-terminus of the Fc region to retain the recombinant proteins within the endoplasmic reticulum (ER).

The analysis of subunit proteins confirmed the average mass and glycosylation of plant-produced V_{HH}-αNTX-Fc and V_{HH}-PLA2-Fc proteins. As shown in Fig. 5, the deconvoluted MS spectrum showed peaks of non-glycosylated, Man7GlcNAc2, Man8GlcNAc2 and Man9GlcNAc2 containing forms. The experimental masses of non-glycosylated V_{HH}-αNTX-Fc and V_{HH}-PLA2-Fc were 41,437.3437 and 41,427.9122 Da, respectively. These masses were 1.37- and 0.82-Da different from their theoretical masses of 41,438.7122 and 41,428.7340 Da, respectively. Man8GlcNAc2 was the most predominant glycosylated form of V_{HH}-αNTX-Fc and V_{HH}-PLA2-Fc. Their experimental masses of 43,141.3079 and 43,131.7045 Da, respectively. The other high-mannose forms, such as Man5GlcNAc2, Man7GlcNAc2 and Man9GlcNAc2, were also observed with mass increases of 1218, 1541 and 1865 Da from their non-glycosylated forms, respectively (Fig. 5).

The protein sequences of the plant-produced V_{HH}-αNTX-Fc and V_{HH}-PLA2-Fc proteins were confirmed by peptide mapping analysis. The resulting peptides sequence obtained were subjected to pBLAST with the NCBI database sequences that were submitted from United States patent published No. US 2013/0259864 A1' Cluster II C2 [32] for the V_{HH}-αNTX region and the Chavanayarn et al., 2012 study [12] for the V_{HH}-PLA2 region. The Fc region of human IgG1 without the CH1 domain (Genbank accession number: 4CDH_A) and a peptide linker GSGGGGSGGGGSGGGGS were used for BLASTP. Most of the peptide sequences were identified by MS/MS profiling, except for GQPREPQ-VYTLPPSRDELTK at the Fc regions of V_{HH}-αNTX-Fc and V_{HH}-PLA2-Fc

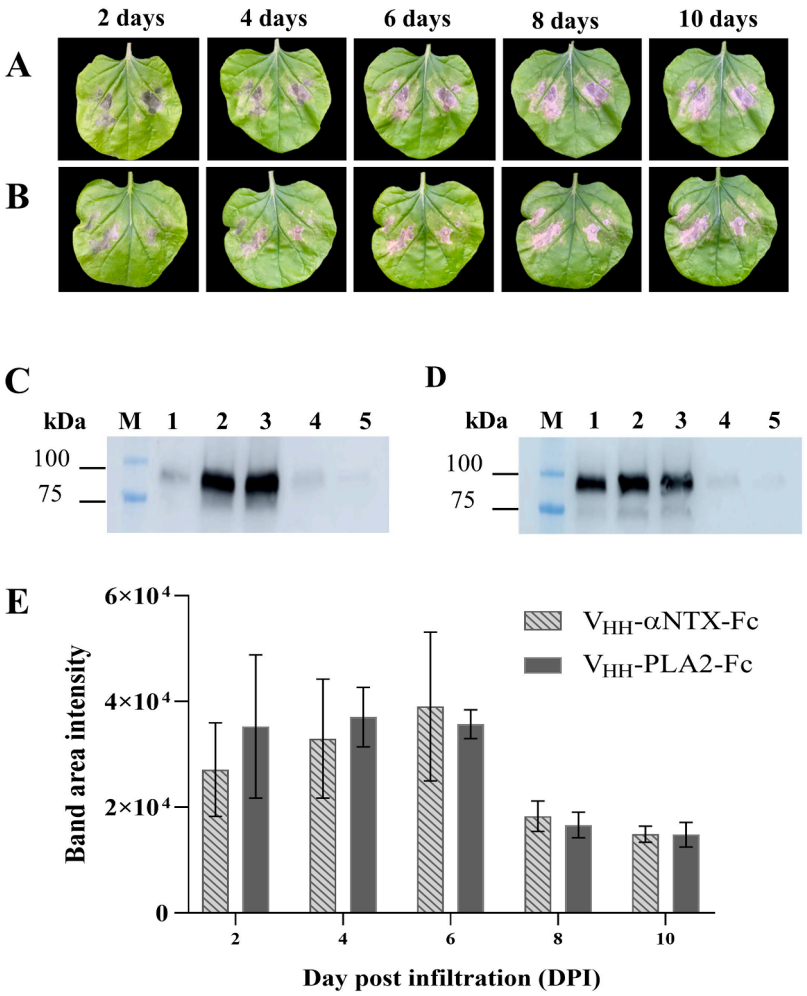

Fig. 3. Determination of expression by days post-infiltration. Leaf necrosis of V_{HH}-αNTX-Fc (A) and V_{HH}-PLA2-Fc (B) observed on day 2, 4, 6, 8 and 10 after infiltration. Western blot analysis was used to quantify the abundance of specific proteins. Western blot of crude extracts of V_{HH}-αNTX-Fc (C) and V_{HH}-PLA2-Fc (D). M: Marker (Bio-Rad, California, USA); lane 1 - 5: crude extracts of day 2, 4, 6, 8, and 10, respectively. (E) Each lane was examined for band intensity to compare the expression level of the target protein using ImageQuant™. The relative amount of band intensity of V_{HH}-αNTX-Fc and V_{HH}-PLA2-Fc production from Western blot analysis. Data are presented as mean ± SD (n = 3).

proteins (Supplemental Figs. S5(A) and S6(A)). The sequence coverages of MS/MS peptides for V_{HH}-αNTX-Fc and V_{HH}-PLA2-Fc were 94.74 % and 94.72 %, respectively. The peptides with the sequence EEQYNSTYR of both V_{HH}-αNTX-Fc and V_{HH}-PLA2-Fc were found to attach with high-mannose glycans, such as Man5GlcNAc2 and Man7GlcNAc2 (see Supplemental Figs. S5(B) and S6(B) and Table S1 and S2). This peptide mapping result confirmed the analyses of the intact and subunit proteins, demonstrating that plant-produced V_{HH}-Fc fusion proteins were glycosylated with high-mannose glycans.

3.4. Investigation of V_{HH}-αNTX-Fc and V_{HH}-PLA2-Fc by antigen-binding ELISA

ELISA was used to assess the binding affinity of purified plant-produced V_{HH}-αNTX-Fc and V_{HH}-PLA2-Fc to crude cobra venom antigens. Both plant-produced V_{HH}-Fcs showed binding to the venom (Fig. 6). However, V_{HH}-αNTX-Fc exhibited a higher binding ability to crude cobra venom in comparison to V_{HH}-PLA2-Fc. The dissociation constant K_d values for plant-produced V_{HH}-αNTX-Fc and V_{HH}-PLA2-Fc were of 0.03038 and 0.7675, respectively.

4. Discussion

The cobra snake (genus: *Naja*) is a venomous reptile found in Asia and Africa that can cause severe snake bites [34,35]. The cobra venom is composed mainly of αNTX and PLA2, which are highly abundant and toxic [36,37]. These postsynaptic (αNTX) and presynaptic PLA2 neurotoxins can cause acute severity, disability, and even death in case of cobra envenomation [5,38,39]. Traditional therapeutic antibodies are typically produced using mammalian cells from horses. However, horse serum antivenom can cause adverse reactions, which can potentially be lethal [40]. Additionally, around 70 % of traditional antivenoms are not directly against the specific venom composition [4]. Moreover, conventional antivenoms are ineffective to treat snake bites at the snake bite site due to their inability to penetrate deeper tissues [41,42]. Previous studies have shown that V_{HH} attached to the Fc fragment can promote effector functions and enhance the neutralization of the toxin [43]. Heavy-chain only antibodies combine the advantages of single variable domains and Fc regions, allowing for rapid penetration [12,16,17,20,44] and prolonged half-life [43,45]. Moreover, the plant-based monoclonal antibody production platform offers many outstanding capabilities to address these challenges. Thus, the possibility of producing antivenom using plant platforms has been further investigated.

In this study, the V_{HH} region was fused with the constant region of the human IgG1 heavy chain (CH_2 and CH_3 domains) and cloned into the geminiviral vector pBY2eK. Both V_{HH}-αNTX-Fc and V_{HH}-PLA2-Fc showed the highest expression levels in *N. benthamiana* leaves on day 6. After day 6, the leaves exhibited more necrosis and produced lower

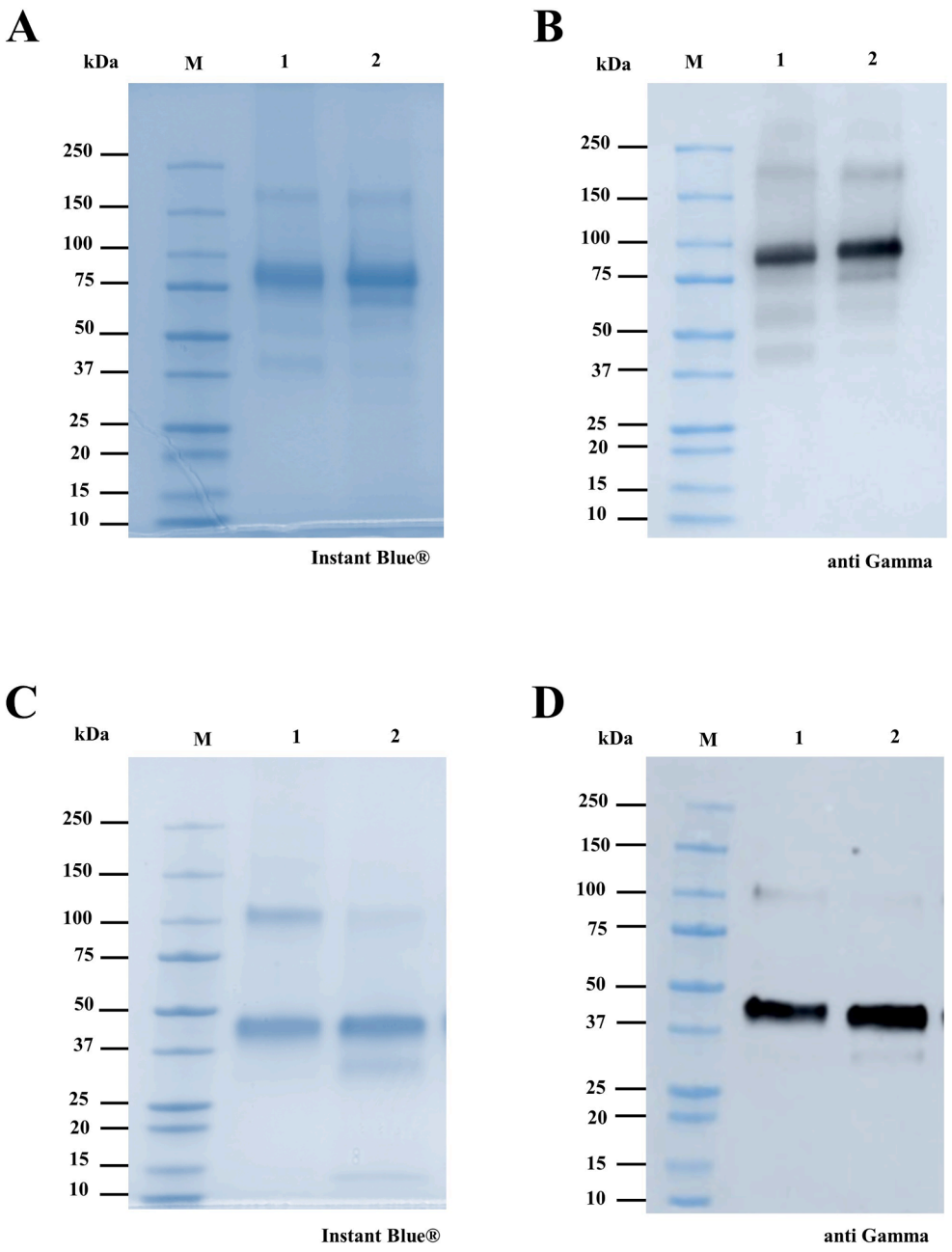

Fig. 4. SDS-PAGE and Western blot analysis of purified plant-produced V_{HH}-αNTX-Fc and V_{HH}-PLA2-Fc. Purified plant-produced V_{HH}-Fc was assessed by SDS-PAGE and Western blot under non-reducing conditions (A and B) and reducing conditions (C and D). Purified proteins were separated on 4–15 % SDS-PAGE and stained with Instant Blue®. For Western blot analysis, the proteins were transferred to nitrocellulose membranes and probed with horseradish peroxidase (HRP)-conjugated goat anti-human IgG (anti Gamma). M: Marker (Bio-Rad, California, USA); Lane 1: Purified plant-produced V_{HH}-αNTX-Fc; Lane 2: Purified plant-produced V_{HH}-PLA2-Fc.

amounts of the target proteins. The results suggest that longer incubation periods after infiltration of *N. benthamiana* may lead to the accumulation of recombinant proteins, leaf necrosis and dehydration [46, 47]. This finding is consistent with previous studies where the leaves exhibited necrosis and a reduction in antibody expression within 1 week [48]. The plant produced V_{HH}-αNTX-Fc and V_{HH}-PLA2-Fc were purified and characterized using SDS-PAGE and Western blotting. Results were consistent with previous studies that produced V_{HH}-Fc proteins capable of neutralizing the α-cobratoxin from *Naja kaouthia* [22].

According to the peptide mapping data, the matched peptides were searched with a mass accuracy of 5 ppm. The MS/MS results confirmed the peptide sequence of V_{HH}-Fc. The MS/MS results of the trypsin digest yielded 94.74 % sequence coverage of V_{HH}-αNTX-Fc and 94.72 % of V_{HH}-PLA2-Fc. Based on, intact mass protein characterization, molecular mass of the assembled V_{HH}-Fc was around 82.8 – 86.6 kDa. This may be of an advantage *in vivo* applications as its molecular weight is above the glomerular filtration cutoff size at 65 kDa. This could lead to extended periods of antibody circulation in human body [20]. The N-glycan characterization profiles revealed that both proteins exhibit high-mannose N-glycans which are typical for glycoproteins retained in the ER of plants [49–52]. Retaining antibodies in the ER has the potential to improve the efficiency of antibody assembly and decrease the chance of accumulating misfolded proteins. This plays a role in achieving increased yields of antibodies that are both correctly folded and functionally active [53]. Moreover, the addition of KDEL to the C-terminus of proteins retained in the ER is a strategy to control the

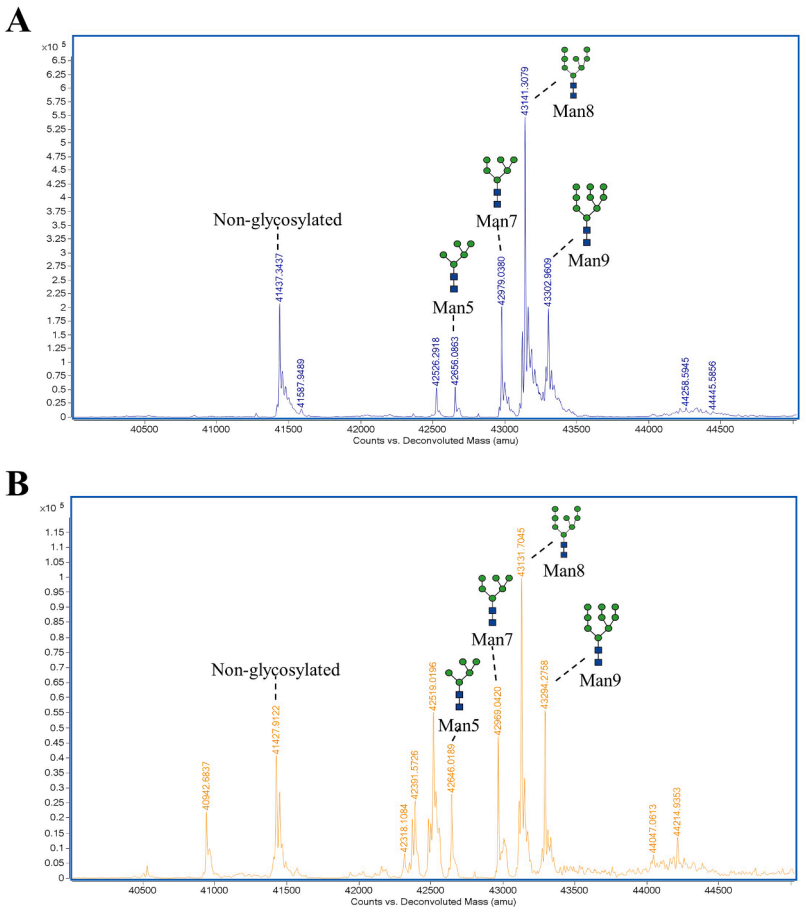

Fig. 5. MS analysis of plant-produced subunit proteins V_{HH}-αNTX-Fc (A) and V_{HH}-PLA2-Fc (B). Peaks corresponding to non-glycosylated V_{HH}-Fc protein and peaks corresponding to V_{HH}-Fc protein carrying the predominant high-mannose N-glycans are indicated. Symbols for glycan illustration (green, mannose; blue, N-acetylglucosamine) are according to the nomenclature from the Consortium for Functional Glycomics.

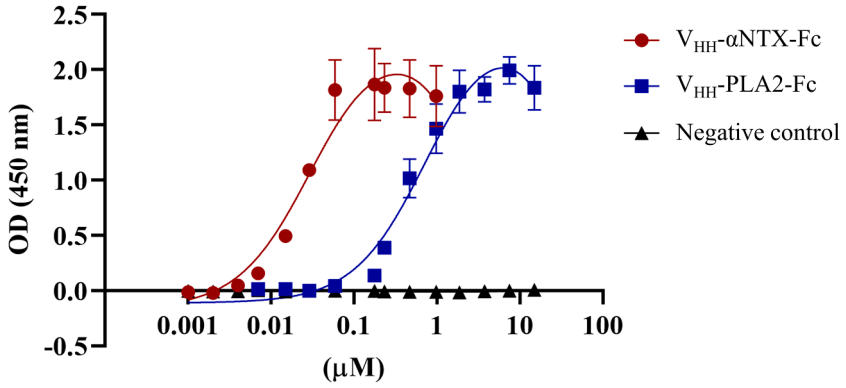

Fig. 6. *In vitro* binding of purified plant-produced V_{HH}-αNTX-Fc and V_{HH}-PLA2-Fc to cobra venom. The binding affinity to the antigen was determined by ELISA. Two-fold dilutions of the plant-produced V_{HH}-αNTX-Fc and V_{HH}-PLA2-Fc proteins were incubated on plates coated with crude cobra venom (*Naja kaouthia*). Plant-produced Pembrolizumab antibody was used as a negative control [33]. A positive control was not used in the study due to the lack of standardization and absence of commercial anti-cobra serum with Fc region, that can bind to the secondary antibody. The bound protein was detected with HRP-conjugated goat anti-human IgG. The data represent the mean ± SD of triplicate assays for each concentration of V_{HH}-Fc.

glycosylation pattern of these proteins, specifically favoring the production of oligomannose-type glycans and avoiding the formation of particular glycoepitopes. This modification can have implications for the functionality, localization, and immunogenicity of the modified proteins [54]. However, glycosylation of the Fc region can differentially affect the antibody functions, receptor-binding properties and pharmacokinetics in human body [55]. Recombinant mAbs with high-mannose N-glycans are reported with increased immunogenicity and faster clearance rate [56], implicating that, the use of plant-produced V_{HH}-Fc antivenoms would require further pharmacokinetic and pharmacodynamic studies and monitoring. The ELISA results showed that V_{HH}-αNTX-Fc has a greater ability to bind to crude venom of *Naja kaouthia* compared to V_{HH}-PLA2-Fc. The difference in binding affinity was due to the presence of higher amounts of α-neurotoxin in elapid species venom compared to phospholipase A2 [7,36]. This implies the interaction of αNTX and PLA2 in the venom composition with varying

affinities or specificities. The dissociation constant (Kd) values provide quantitative insights into the binding affinities of the proteins. A lower Kd value indicates stronger binding affinity. In this case, the Kd value for plant-produced V_{HH}-αNTX-Fc was found to be 0.03038, indicating a relatively high affinity for the venom components. Conversely, the Kd value for V_{HH}-PLA2-Fc was higher at 0.7675, suggesting a lower affinity for the venom. These differences in binding affinity could have significant implications for the efficacy and application of these constructs in various contexts, such as therapeutic interventions or diagnostic assays. Constructs with higher affinity, like V_{HH}-αNTX-Fc, may be more effective in neutralizing venom toxins or detecting venom components with greater sensitivity. However, the difference in binding ratios between V_{HH}-αNTX-Fc and V_{HH}-PLA2-Fc may indeed be attributed to the composition of crude cobra venom, which likely contains a higher concentration of alpha-neurotoxin compared to phospholipase A2. This difference in venom composition could account for the varying affinities observed between the two V_{HH}-Fc constructs.

5. Conclusions

In summary, our studies have shown that *Nicotiana benthamiana* can produce the target proteins V_{HH}-αNTX-Fc and V_{HH}-PLA2-Fc with the highest level of expression within one week. Our findings show that plant-produced V_{HH}-αNTX-Fc and V_{HH}-PLA2-Fc have the ability to bind to crude cobra venom (*Naja kaouthia*). This study offers advantages for the development of an alternative treatment against cobra venom with no limitations in comparison with traditional serum-based therapies and potentially lower production costs. However, further studies are required to determine the *in vivo* neutralization and improve the stability of plant-produced V_{HH}-αNTX-Fc and V_{HH}-PLA2-Fc as anti-cobra venom.

Funding

This study received financial support from the Second Century Fund (C2F), Chulalongkorn University, the NSRF via the Program Management Unit for Human Resources & Institutional Development, Research, and Innovation [grant number B13F660137], and the 90th Anniversary of Chulalongkorn University "Rachadapisek Sompote Fund" and Baiya Phytopharm Co., Ltd.

CRediT authorship contribution statement

Sarocha Vitayathikornnasak: Writing – review & editing, Writing – original draft, Methodology, Conceptualization. **Kaewta Rattanapisit:** Formal analysis, Investigation, Methodology. **Ashwini Malla:** Writing – review & editing. **Pipob Suwanchaikasem:** Formal analysis, Validation. **Richard Strasser:** Writing – review & editing. **Narach Khorattanakulchai:** Formal analysis, Investigation, Methodology. **Kanokporn Pothisamutyothin:** Methodology. **Wanatchaporn Arunmanee:** Conceptualization, Supervision, Project administration. **Waranyoo Phoolcharoen:** Conceptualization, Supervision, Project administration.

Declaration of competing interest

WP from Chulalongkorn University is a founder/shareholder of Baiya Phytopharm Co., Ltd. Thailand.

Data availability

Data will be made available on request.

Acknowledgments

The author (S.V.) is a recipient of 'The Second Century Fund (C2F)' scholarship of Chulalongkorn University. The project was also supported by the NSRF via the Program Management Unit for Human Resources & Institutional Development, Research, and Innovation [grant number B13F660137], and the 90th Anniversary of Chulalongkorn University "Rachadapisek Sompote Fund".

Supplementary materials

Supplementary material associated with this article can be found, in the online version, at doi:10.1016/j.btre.2024.e00841.

References

[1] World Health Organization, W. *Prevalence of snakebite envenoming*. N.D. [cited 2023 April 14, 2023]; Available from: https://www.who.int/teams/control-of-neglected-tropical-diseases/snakebite-envenoming/prevalence.
[2] World Health Organization. *Regional Action Plan for prevention and control of snakebite envenoming in South-East Asia 2022–2030 published in New Delhi*. 2023 [cited 2023 April 14, 2023]; Available from: https://www.who.int/news/item/05-02-2023-regional-action-plan-for-prevention-and-control-of-snakebite-envenoming-in-south-east-asia-2022-2030.
[3] K. Ratanabanangkoon, A Quest for a universal plasma-derived antivenom against all elapid neurotoxic snake venoms, Front. Immunol. 12 (2021).
[4] A.H. Laustsen, et al., Pros and cons of different therapeutic antibody formats for recombinant antivenom development, Toxicon 146 (2018).
[5] B. Kalita, Y.N. Utkin, A.K. Mukherjee, Current insights in the mechanisms of cobra venom cytotoxins and their complexes in inducing toxicity: implications in antivenom therapy, Toxins (Basel) 14 (839) (2022).
[6] Y.N. Utkin, A.V. Osipov, Non-lethal polypeptide components in cobra venom, Curr. Pharmaceut. Des. 13 (28) (2007) 2906–2915.
[7] A.L. Oliveira, et al., The chemistry of snake venom and its medicinal potential, Nat. Rev. Chem. 6 (7) (2022) 451–469.
[8] T. Lynagh, et al., Peptide inhibitors of the α-cobratoxin−nicotinic acetylcholine receptor interaction, J. Med. Chem. 63 (22) (2020).
[9] C.-C. Liu, et al., Analysis of the efficacy of Taiwanese freeze-dried neurotoxic antivenom against Naja kaouthia, Naja siamensis and Ophiophagus hannah through proteomics and animal model approaches, PLoS Negl Trop. Dis. 11 (12) (2017) e0006138.
[10] A. Osipov, Y. Utkin, What Are the Neurotoxins in Hemotoxic Snake Venoms? Int. J. Mol. Sci. 24 (3) (2023) 2919.
[11] C.R. Ferraz, et al., Multifunctional Toxins in Snake Venoms and Therapeutic Implications: from Pain to Hemorrhage and Necrosis, Front. Ecol. Evol. 7 (2019).
[12] C. Chavanayarn, et al., Humanized-Single Domain Antibodies (VH/VHH) that Bound Specifically to Naja kaouthia Phospholipase A2 and Neutralized the Enzymatic Activity, Toxins (Basel) 4 (2012).
[13] P.E. Bickler, Amplification of Snake Venom Toxicity by Endogenous Signaling Pathways, Toxins (Basel) 12 (68) (2020).
[14] S.R. Sudulagunta, et al., Cardiotoxicity and respiratory failure due to Cobra bite, Appl. Med. Sci. 3 (5A) (2015) 1830–1833.
[15] B.K. Jin, et al., Nanobodies: a review of generation, diagnostics and therapeutics, Int. J. Mol. Sci. 24 (6) (2023).
[16] C.S. Bever, et al., VHH antibodies: emerging reagents for the analysis of environmental chemicals, Anal. Bioanal. Chem. 408 (2016).
[17] P. Bannas, J. Hambach, F. Koch-Nolte, Nanobodies and nanobody-based human heavy chain antibodies as antitumor therapeutics, Front. Immunol. 8 (2017).
[18] M.M. Harmsen, H.J. De Haard, Properties, production, and applications of camelid single-domain antibody fragments, Appl. Microbiol. Biotechnol. 77 (1) (2007) 13–22.
[19] S. Kunz, et al., NANOBODY® Molecule, a Giga Medical Tool in Nanodimensions, Int. J. Mol. Sci. 24 (17) (2023) 13229.
[20] Y. Asaadi, et al., A comprehensive comparison between camelid nanobodies and single chain variable fragments, Biomark. Res. 9 (87) (2021).
[21] Demarco, S. *Snakebite antivenoms step into the future*. 2022. 18.
[22] G. Richard, et al., In Vivo Neutralization of α-Cobratoxin with High-Affinity Llama Single-Domain Antibodies (V_HHs) and a V_HH-Fc Antibody, PLoS ONE 8 (7) (2013).
[23] S. Nosaki, et al., Transient protein expression systems in plants and their applications, Plant Biotechnol. 38 (2021).
[24] K.B. Moon, et al., Development of Systems for the Production of Plant-Derived Biopharmaceuticals, Plants 9 (30) (2020).
[25] J.K.-C. Ma, et al., Regulatory approval and a first-in-human phase I clinical trial of a monoclonal antibody produced in transgenic tobacco plants, Plant Biotechnol. J. 13 (2015).
[26] T.V. Komarova, et al., Plant-Made Trastuzumab (Herceptin) Inhibits HER2/Neu+ Cell Proliferation and Retards Tumor Growth, PLoS ONE 6 (3) (2011).
[27] K. Rattanapisit, et al., Plant-Produced Anti-Enterovirus 71 (EV71) Monoclonal Antibody EV71 Infection, Plants 8 (2019).
[28] M.-A. D'Aoust, et al., Influenza virus-like particles produced by transient expression in Nicotiana benthamiana induce a protective immune response against a lethal viral challenge in mice, Plant Biotechnol. J. 6 (9) (2008) 930–940.
[29] B. Lumlertdacha, et al., Efficiency Comparative Approach of Plant-Produced Monoclonal Antibodies against Rabies Virus Infection, Vaccines (Basel) 11 (8) (2023).

[30] J.G. Park, et al., A Broad and Potent H1-Specific Human Monoclonal Antibody Produced in Plants Prevents Influenza Virus Infection and Transmission in Guinea Pigs, Viruses 12 (2) (2020).
[31] M. Knödler, et al., Design, optimization, production and activity testing of recombinant immunotoxins expressed in plants and plant cells for the treatment of monocytic leukemia, Bioengineered 14 (1) (2023) 2244235.
[32] Hall, J.C., G. Richard, and M.D. McLean, *Anti-Cobra Toxin antibody fragments and method of producing a VHH library*. 2013: United States. p. 31.
[33] T. Phakham, et al., Functional Characterization of Pembrolizumab Produced in Nicotiana benthamiana Using a Rapid Transient Expression System, Front. Plant. Sci. 12 (2021).
[34] Organization, W.H. *Snakes gallery*. 2023 [cited 2023 23-Jul-23]; Available from: https://www.who.int/teams/control-of-neglected-tropical-diseases/snakebite-envenoming/snakes-gallery.
[35] M.A.W. Chowdhury, J. Müller, S. Varela, Climate change and the increase of human population will threaten conservation of Asian cobras, Sci. Rep. 11 (1) (2021).
[36] K.Y. Tan, et al., Venomics, lethality and neutralization of Naja kaouthia (monocled cobra) venoms from three different geographical regions of Southeast Asia, J. Proteomics 120 (2015) 105–125.
[37] J.M. Gutiérrez, et al., The Search for natural and synthetic inhibitors that would complement antivenoms as therapeutics for snakebite envenoming, Toxins (Basel) 13 (7) (2021) 451.
[38] H. Xiao, et al., *Snake Venom* PLA_2, *a Promising target for broad-spectrum antivenom drug development*, Biomed. Res. Int. 2017 (2017) 1–10.
[39] U.K. Ranawaka, D.G. Lalloo, H.J. De Silva, Neurotoxicity in snakebite—the limits of our knowledge, PLoS Negl. Trop. Dis. 7 (10) (2013) e2302.
[40] I. Nuchprayoon, P. Garner, Interventions for preventing reactions to snake antivenom, Cochr. Datab. Syst. Rev. (1999).
[41] J. MARIÂ, et al., Neutralization of local tissue damage induced by Bothrops asper (terciopelo) snake venom, Toxicon 36 (11) (1998).
[42] G. Bao, et al., Nanobody: a promising toolkit for molecular imaging and disease therapy, EJNMMI Res. 11 (1) (2021).
[43] Godakova, et al., Camelid VHHs Fused to Human Fc fragments provide long term protection against botulinum neurotoxin a in mice, Toxins (Basel) 11 (8) (2019) 464.
[44] S.C. Clarke, et al., Multispecific antibody development platform based on human heavy chain antibodies, Front. Immunol. 9 (2019).
[45] V. Bobkov, et al., Nanobody-Fc constructs targeting chemokine receptor CXCR4 potently inhibit signaling and CXCR4-mediated HIV-entry and induce antibody effector functions, Biochem. Pharmacol. 158 (2018) 413–424.
[46] X. Zhang, et al., Transcriptomic and metabolomic investigation on Leaf Necrosis Induced by ZmWus2 transient overexpression in nicotiana benthamiana, Int. J. Mol. Sci. 24 (13) (2023) 11190.
[47] S. Nosaki, et al., Prevention of necrosis caused by transient expression in Nicotiana benthamiana by application of ascorbic acid, Plant Physiol. 186 (2) (2021) 832–835.
[48] N. Kaewbandit, et al., Effect of plant produced Anti-hIL-6 receptor antibody blockade on pSTAT3 expression in human peripheral blood mononuclear cells, Sci. Rep. 13 (1) (2023) 11927.
[49] B. Balen, M. Krsnik-Rasol, N-glycosylation of recombinant therapeutic glycoproteins in plant systems, Food Technol. Biotechnol. 45 (1) (2007).
[50] S. Boune, et al., Principles of N-linked glycosylation variations of IgG-based therapeutics: pharmacokinetic and functional considerations, Antibodies 9 (2) (2020) 22.
[51] C.J.I. Bulaon, et al., Antitumor effect of plant-produced anti-CTLA-4 monoclonal antibody in a murine model of colon cancer, Front Plant Sci. 14 (2023) 1149455.
[52] H.-S. Kim, et al., N-Glycosylation Modification of Plant-derived Virus-Like Particles: an application in vaccines, Biomed. Res. Int. 2014 (2014) 249519.
[53] S. Petruccelli, et al., A KDEL-tagged monoclonal antibody is efficiently retained in the endoplasmic reticulum in leaves, but is both partially secreted and sorted to protein storage vacuoles in seeds, Plant Biotechnol. J. 4 (5) (2006) 511–527.
[54] J.-H. Lee, et al., Intracellular reprogramming of expression, glycosylation, and function of a plant-derived antiviral therapeutic monoclonal antibody, PLoS ONE 8 (8) (2013) e68772.
[55] L.L. Lu, et al., Beyond binding: antibody effector functions in infectious diseases, Nat. Rev. Immunol. 18 (1) (2018) 46–61.
[56] Y. Durocher, M. Butler, Expression systems for therapeutic glycoprotein production, Curr. Opin. Biotechnol. 20 (6) (2009) 700–707.